Available online at www.sciencedirect.com
ScienceDirect
International Journal of Heat and Fluid Flow 29 (2008) 1174–1181
International Journal of HEAT AND FLUID FLOW
www.elsevier.com/locate/ijhff

Numerical study of natural convection dominated heat transfer in a ventilated cavity: Case of forced flow playing simultaneous assisting and opposing roles

A. Raji [a,*], M. Hasnaoui [b], A. Bahlaoui [a]

[a] Faculty of Sciences and Technologies, Department of Physics, University Sultan Moulay Slimane, Team of Flows and Transfers Modeling (EMET), Laboratory of Physics and Mechanics of Materials, B.P. 523, Béni-Mellal, Morocco
[b] Faculty of Sciences Semlalia, Department of Physics, University Cadi Ayyad, UFR TMF, B.P. 2390 Marrakesh, Morocco

Received 1 June 2007; received in revised form 10 January 2008; accepted 28 January 2008
Available online 10 March 2008

Abstract

Mixed convection heat transfer in a ventilated cavity is numerically studied by solving the mixed convection equations with the Boussinesq approximation. Results are presented in terms of streamlines, isotherms and heat transfer for different combinations of the governing parameters namely, the Reynolds number ($10 \leqslant Re \leqslant 5000$), the Rayleigh number ($10^4 \leqslant Ra \leqslant 10^6$) and the relative height of the openings ($B = h'/H' = 1/4$). The numerical results show the presence of a maximum interaction between the effects of the forced and natural convection and the existence of different flow regimes. The latter are delineated in the *Ra*–*Re* plane and the values of *Re* separating the different regions are determined and correlated versus *Ra*.

Keywords: Mixed convection; Ventilated cavity; Numerical study; Heat transfer; Correlations

1. Introduction

Mixed convection in ventilated cavities has received a sustained attention, due to the interest of the phenomenon in many technological processes, such as the design of solar collectors, thermal design of buildings, air conditioning and, recently, the cooling of electronic circuit boards. In ventilated enclosures, the interaction between the external forced stream and the buoyancy driven flow induced by buoyancy forces could lead to complex flow structures. A literature review on the subject shows that many authors have considered mixed convection in ventilated enclosures. Oosthuizen and Paul (1985) studied numerically mixed convection heat transfer in a cavity with uniformly heated isothermal vertical walls and horizontal adiabatic walls. The forced flow was considered either aiding or opposing to the buoyancy force effect. The cold wall was provided by two openings for the admission and the evacuation of the forced stream. Papanicolaou and Jaluria (1990, 1993) studied numerically the mixed convection transport from an isolated heat source with a uniform heat flux input within a rectangular enclosure. Their results showed that the average Nusselt number increases by increasing the Richardson/(Reynolds) number at a fixed Reynolds/(Richardson) number. Also, the heat transfer was found to increase by increasing the solid wall thermal conductivity. Later on, the same authors (Papanicolaou and Jaluria, 1994) studied mixed convection in a ventilated rectangular cavity containing heat sources. The results presented show that the interaction between the sources is strongly dependent on their relative locations in the enclosure and their height. A sustained oscillatory behavior was obtained for $Gr/Re^2 = 50$. Mixed convection in a square enclosure with

* Corresponding author. Tel.: +212 23 48 51 12/22/82; fax: +212 23 48 52 01.
E-mail addresses: abderaji@fstbm.ac.ma, abderaji@caramail.com (A. Raji).

0142-727X/$ - see front matter © 2008 Elsevier Inc. All rights reserved.
doi:10.1016/j.ijheatfluidflow.2008.01.010

Nomenclature

A	aspect ratio of the cavity ($=L'/H'$)
B	relative height of the openings ($=h'/H'$)
g	acceleration due to gravity (m/s^2)
h'	height of the openings (m)
H'	height of the cavity (m)
L'	total length of the cavity (m)
Nu	normalized mean Nusselt number, Eq. (7)
Pr	Prandtl number, Eq. (6)
q'	dimensional imposed heat flux (W/m^2)
Ra	Rayleigh number, Eq. (6)
Re	Reynolds number, Eq. (6)
t	dimensionless time ($=t'u'_o/H'$)
T	dimensionless fluid temperature ($=(T'-T'_C)/(q'H'/\lambda)$)
T'	dimensional fluid temperature (K)
T'_C	temperature of the imposed cold flow (K)
$\overline{T}$	mean dimensionless temperature
$\overline{T}^*$	modified mean temperature ($=\overline{T}\times Ra$)
T^*_{max}	modified maximum temperature ($=T_{max}\times Ra$)
(u,v)	dimensionless horizontal and vertical velocities ($=(u',v')/u'_o$)
u'_o	dimensional velocity of the imposed flow (m/s)
(x,y)	dimensionless Cartesian coordinates ($=(x',y')/H'$)

Greek symbols

α	thermal diffusivity of fluid (m^2/s)
β	thermal expansion coefficient of fluid (1/K)
λ	thermal conductivity of fluid (W/(K m))
ν	kinematic viscosity of fluid (m^2/s)
Ω	dimensionless vorticity ($=\Omega' H'/u'_o$)
Ψ	dimensionless stream function ($=\Psi'/u'_o H'$)

Subscripts

C	cold
f	forced
m	mixed
max	maximum

Superscript

$'$	dimensional variables

a partially dividing partition was studied numerically by Hsu et al. (1997). The results presented show that the average Nusselt number increases by increasing $Re/(Gr/Re^2)$ for a given value of $Gr/Re^2/(Re)$. Results of the simulations indicate that the heat dissipated from the source is maximum when the outflow opening is placed at the lower part of the vertical wall. A better heat removal was also obtained when the heat source was located as close as possible to the cold stream inlet opening. The case of transient mixed convection in a square enclosure with a partially dividing partition was also studied by How and Hsu (1998). The conducting baffle was placed either on the bottom or the top of the horizontal walls. Results of the study show that the transient heat transfer and fluid flow structure are strongly dependent on the height and location of the baffle and, generally, either higher values of Re or lower values of Gr/Re^2 delay the achievement of the steady state solutions. A numerical study was conducted by Hsu and Wang (2000) on mixed convective heat transfer in an enclosure containing discrete heat sources. The authors found that both the thermal field and the Nusselt number are strongly dependent on the position of the heat sources and their conductivity ratio. Laminar mixed convection in a two-dimensional enclosure with assisting and opposing flows was studied numerically by Raji and Hasnaoui in the case of a cavity uniformly heated from one side wall (1998a) or with prescribed equal heat fluxes on the top horizontal wall and the vertical left one (2000). The obtained results show that the Re–Ra plane can be divided in regions corresponding to the dominance of the forced convection or to the mixed convection regime where the maximum heat transfer (maximum thermal interaction between forced and natural convection) and the limits between both regimes were correlated in terms of Re versus Ra. Manca et al. (2003) studied numerically the effect of the heated wall position on mixed convection in a partially open cavity. The results showed that the maximum temperature values decrease by increasing the Reynolds and the Richardson numbers. Also, the opposing forced flow configuration was found to achieve the highest thermal performance in terms of both maximum temperature and average Nusselt number. Laminar mixed convection in a two-dimensional enclosure, differentially heated, was studied numerically by Singh and Sharif (2003). They reported that maximum cooling effectiveness is achieved if the inlet and the outlet openings are, respectively, located near the bottom of the cold wall and the top of the hot wall. Laminar double diffusion mixed convection in a two-dimensional ventilated enclosure was numerically investigated by Deng et al. (2004). Combined effects of the Grashof number, the Reynolds number, the buoyancy ratio and the ventilation mode on the indoor air environment were examined. A numerical study of laminar mixed convection in a shallow enclosure with a series of block-like heat generating components with floor admission openings and ceiling extraction openings was conducted by Bhoite et al. (2005). They reported that the effect of buoyancy becomes insignificant for $Re > 600$. Combined free convection and forced convection from a flush-mounted uniform heat source on the bottom of a horizontal rectangular enclosure with two exit ports, located at the top of the vertical walls, was recently studied numerically by Saha et al. (2006).

They found that the increase of *Re* or *Gr* value leads to higher heat transfer coefficient, higher heat source temperature and higher intensity of recirculating flow. Useful correlations are proposed for the Nusselt number versus Reynolds and Richardson numbers.

On the basis of the literature review, it appears that no work was reported on mixed convection in a ventilated rectangular enclosure within which both aiding and opposing flow cases are simultaneously encountered. Thereafter, due to its practical interest, the subject needs to be further explored to improve the knowledge in this field. Hence, the aim of the present study consists in studying numerically a mixed convection problem in a ventilated cavity submitted to a constant heat flux on one of its vertical walls. In this analysis, the forced flow enters the cavity through an opening located in the middle of the heated vertical wall and leaves it from an opening located in the opposite adiabatic wall. This kind of ventilation supports a double interaction between the buoyancy-induced flow and the forced flow. In the lower part of the cavity, the forced flow injected in the cavity promotes the natural convection motion while it plays an opposing role vis-à-vis of the natural convection flow developed in the upper part of the cavity. Thus, combined effects of the Rayleigh number and the intensity of the imposed flow (through the Reynolds number) on the flow structure and heat transfer across the cavity is examined for this specific situation.

2. Problem formulation

The configuration under study with the system of coordinates is sketched in Fig. 1. It consists of a ventilated cavity heated by a uniform heat flux from its vertical left wall while the remaining walls are considered perfectly insulated. The system is submitted to an imposed flow of fresh air, parallel to the horizontal walls, entering and leaving the cavity from two opposing openings located at the middle of the vertical plates. The third dimension of the cavity (direction perpendicular to plane of the diagram) is assumed to be large enough so that the fluid motion can be considered two-dimensional. The flow is assumed to be laminar and incompressible with negligible viscous dissipation. All the thermophysical properties of the fluid are assumed constant except the density giving rise to the buoyancy forces (Boussinesq approximation). Taking into account the above-mentioned assumptions, the non-dimensional governing equations, written in $\Omega - \Psi$ formulation, are as follows:

$$\frac{\partial \Omega}{\partial t} + u\frac{\partial \Omega}{\partial x} + v\frac{\partial \Omega}{\partial y} = \frac{1}{Re}\left[\frac{\partial^2 \Omega}{\partial x^2} + \frac{\partial^2 \Omega}{\partial y^2}\right] + \frac{Ra}{Re^2 \mathrm{Pr}}\frac{\partial T}{\partial x} \tag{1}$$

$$\frac{\partial T}{\partial t} + u\frac{\partial T}{\partial x} + v\frac{\partial T}{\partial y} = \frac{1}{Re\mathrm{Pr}}\left[\frac{\partial^2 T}{\partial x^2} + \frac{\partial^2 T}{\partial y^2}\right] \tag{2}$$

$$\frac{\partial^2 \Psi}{\partial x^2} + \frac{\partial^2 \Psi}{\partial y^2} = -\Omega \tag{3}$$

The stream function, Ψ, and the vorticity, Ω, are related to the velocity components by the following expressions:

$$u = \frac{\partial \Psi}{\partial y}, \quad v = -\frac{\partial \Psi}{\partial x} \quad \text{and} \quad \Omega = \frac{\partial \mathrm{v}}{\partial x} - \frac{\partial u}{\partial y} \tag{4}$$

Referring to Fig. 1, the dimensionless variables are

$$x = \frac{x'}{H'}, \quad y = \frac{y'}{H'}, \quad u = \frac{u'}{u'_{\mathrm{o}}}, \quad v = \frac{v'}{u'_{\mathrm{o}}},$$
$$\Psi = \frac{\Psi'}{u'_{\mathrm{o}}H'}, \Omega = \frac{\Omega' H'}{u'_{\mathrm{o}}}, \quad T = \frac{(T' - T'_{\mathrm{C}})}{q'H'/\lambda} \tag{5}$$

The boundary conditions, associated to the problem are

$u = v = 0$ on the rigid walls
$T = \Omega = v = 0$, $u = 1$ and $\Psi = y - (1 - B)/2$ at the inlet of the cavity
$\frac{\partial T}{\partial x} = -1$ on the heated left vertical wall
$\frac{\partial T}{\partial n} = 0$ on the adiabatic walls

"n" being the direction normal to the considered adiabatic wall.

The boundary conditions at the exit of the cavity are unknown for this problem. Values of u, v, T, Ω and Ψ are obtained at each time step by means of an extrapolation technique similar to that used in the past by Yücel et al. (1993) and Raji and Hasnaoui (1998a,b, 2000). This procedure, based on zero second derivatives for all the above-mentioned variables at the exit of the cavity, does not need artificial extension of the calculation domain at the level of the exit.

The dimensionless parameters appearing in Eqs. (1) and (2) are the Prandtl, *Pr*, the Rayleigh, *Ra*, and the Reynolds, *Re*, numbers. They are, respectively, defined as follows:

$$Pr = \nu/\alpha; \quad Ra = g\beta q' H'^4/\lambda\alpha\nu; \quad Re = u'_{\mathrm{o}}H'/\nu. \tag{6}$$

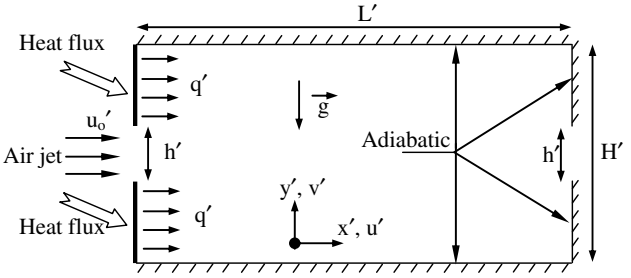

Fig. 1. Schematic of the studied configuration.

3. Heat transfer

The normalized mean Nusselt number, with respect to that of the pure forced convection, evaluated on the heated vertical wall of the cavity, is defined by

$$Nu = \frac{Q(Ra \neq 0)}{Q(Ra = 0)} = \frac{1}{Q(Ra = 0)} \left(\int_0^{0.5-\frac{B}{2}} \frac{1}{T}\bigg|_{x=0} dy + \int_{0.5+\frac{B}{2}}^{1} \frac{1}{T}\bigg|_{x=0} dy \right). \quad (7)$$

4. Numerical method

The governing equations were discretized by using a finite difference technique. Eqs. (1) and (2) were solved by adopting the Alternating Direction Implicit scheme (ADI). Values of the stream function at all grid points were obtained with Eq. (3) by means of the Point Successive Over-Relaxation method (PSOR) with an optimum over-relaxation coefficient equal to 1.88 for the considered grid. At each time step, a variation by less than 10^{-5} over all the grid points for the stream function is considered as the convergence criterion. A further decrease of this value did not cause any significant change in the results. The first and second derivatives of the diffusive terms were approached by central differences while a second order upwind scheme was used for the convective terms to avoid possible instabilities frequently encountered in mixed convection problems. As a result of a grid independence study, a uniform grid size of 81×41 was found to model accurately the flow fields and heat transfer characteristics within the studied configuration. In fact, a refinement of the mesh to 121×61 leads to maximum differences less than 0.8% and 0.2%, respectively, in terms of the Nusselt number and maximum stream function. The accuracy of the numerical model was also checked by comparing the results from the present study with those obtained by De Vahl Davis (1983) for natural convection in a differentially heated cavity and against the results obtained by Yücel et al. (1993) in the case of an inclined ventilated channel discretely heated from one side. The relative differences, observed in terms of Nu and Ψ_{max}, calculated for various combinations of the governing parameters, are found to agree within 1.6% and 1.24%, respectively (Table 1). Finally, for all the computations, it was carefully verified that the balance of heat (the quantity of heat provided to the fluid by the heated wall compared to that leaving the cavity through the exit) is satisfied with 0.2% as a maximum difference.

5. Results and discussion

In the following, effects of the Rayleigh number ($10^4 \leqslant Ra \leqslant 10^6$) and the Reynolds number ($10 \leqslant Re \leqslant 5000$) on the fluid flow and the temperature distribution are illustrated. It t should be noted that the upper value considered for Re ($Re = 5000$) is imposed by the fact that the height H′ of the cavity is considered as a characteristic length instead of the height h' of the openings. In addition, the Reynolds number, Re^*, based on h', is more appropriate to characterize the flow regime (laminar or turbulent) than that based on H'. The maximum value reached by Re^* is $Re \times (h'/H') = 1250$ which guarantees a laminar flow for the studied problem. The calculations were conducted by considering air as a working fluid ($Pr = 0.72$). The aspect ratio, $A = L'/H'$, and the relative height of the openings, $B = h'/H'$, are maintained constant at 2 and 1/4, respectively.

Table 1
Effect of Ra on Ψ_{max} and Nu in the case of an inclined channel discreetly heated from below for $\theta = 30°$, $Re = 10$ and $A = 10$

	$Ra = 5 \times 10^3$		$Ra = 10^4$		$Ra = 10^5$	
	Ψ_{max}	Nu	Ψ_{max}	Nu	Ψ_{max}	Nu
Present work	1.480	1.371	2.232	1.622	10.379	3.519
Yücel et al. (1993)	1.480	1.375	2.227	1.625	10.276	3.450

Results of the study were obtained for values of the Richardson number ($Ri = Ra/(Re^2 Pr)$), varying from 5.5×10^{-4} to 1.4×10^4. This range of Ri was selected on the basis of preliminary calculations covering natural-convection, mixed-convection, and forced-convection dominating regimes. For weak values of Ri, the forced convection regime is dominant. For $Ri \geqslant 1.4 \times 10^4$, numerical instabilities were observed. These instabilities were expected in the natural convection dominating regime. In fact, the boundary conditions imposed at the inlet of the cavity become not compatible with the physical nature of the problem when natural convection is largely dominating; big closed cells are formed inside the cavity and prevent the free circulation of the imposed flow characterized by the open lines.

The effect of the Reynolds number on the flow structure and temperature distribution is shown in Fig. 2a–e. The streamlines and the isotherms are presented for steady state flows obtained for $Ra = 10^6$ and values of the Reynolds number ranging between 20 and 5000. For $Re = 20$, the analysis of the streamlines in Fig. 2a reveals a complex structure in the upper part of the cavity where the presence of two counter-rotating cells is observed. The lower cell is located just in front of the entry opening, above the open lines, and its presence is imposed by the upper cell. In fact, the heated portion of the left wall, located above the opening, imposes a clockwise circulation, but at low Re where the natural convection effect is important, the clockwise circulation of the upper cell is physically impossible without formation of a counter-clockwise rotating cell just below it. Fig. 2a examination shows also the existence of a small convective cell clockwise rotating and located in the vicinity of the left lower corner of the cavity. Being absent in the basic flow, its existence is only due to the effect of natural convection. The distribution of the temperature field shows that the lower part of the cavity (far from the heated wall) is at the temperature of the external flow. The lower cell will play an increasingly important role by increasing Re since more intense is the forced flow, more important is its negative (positive) effect on the natural convection flow in the upper (lower) part of the cavity. This tendency is already visible in Fig. 2b for $Re = 50$. In fact, it is clearly visible from Fig. 2b that this relatively limited increase of

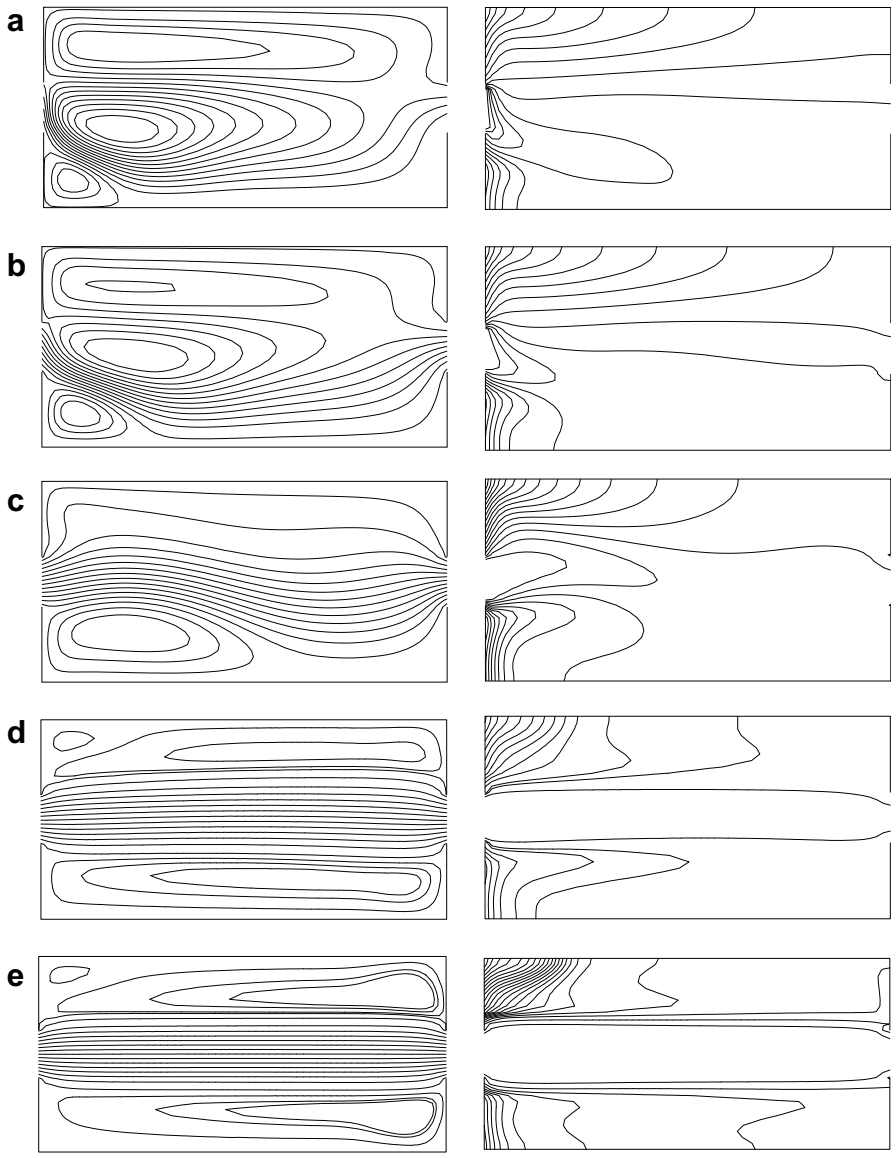

Fig. 2. Streamlines and isotherms obtained for $Ra = 10^6$ and different values of Re: (a) $Re = 20$, (b) $Re = 50$, (c) $Re = 150$, (d) $Re = 1178.51$ and (e) $Re = 5000$.

Re is accompanied by a reduction of the size and the intensity of the upper cells in favor of the open lines and the tendency is supported by the increase of Re until the total disappearance of the upper closed cells which occurs when the intensity of the forced flow reaches a critical value (not given here). Indeed, the role played by natural convection is weakened (supported) in the upper (lower) part of the cavity by increasing Re. When the forced flow overcomes the effect of natural convection in the upper part of the cavity, the open lines are aspired by the heated surface above the aperture as indicated in Fig. 2c for $Re = 150$. The corresponding isotherms are more tightened at the vicinity of the heated wall testifying of a noticeable increase in convective heat exchange. In addition, a net progression of the cold zone towards the right wall is observed. A further increase of the Reynolds number acts in increasing the aiding role of forced and natural convection in the lower part of the cavity. Hence, the intensification of the forced flow leads to an increase of the role played by the lower cell as shown in Fig. 2d–e, respectively, for $Re = 1178.51$ ($Ri = 1$) and $Re = 5000$ ($Ri = 0.055$). It can also be seen that the forced flow crosses directly the cavity from an opening to the other without being constrained to go along the heated upper wall before reaching the exit, which favors the formation of two recirculating cells of different sizes in the upper part of the cavity. The analysis of the isotherms shows that the central part of the cavity is maintained isothermal and cold due to the absence of thermal interaction between the forced flow and the heated boundaries.

The effect of the Rayleigh number on the flow structure and temperature distribution inside the cavity is illustrated in Fig. 3a–d for $Re = 10$ and four selected values of Ra.

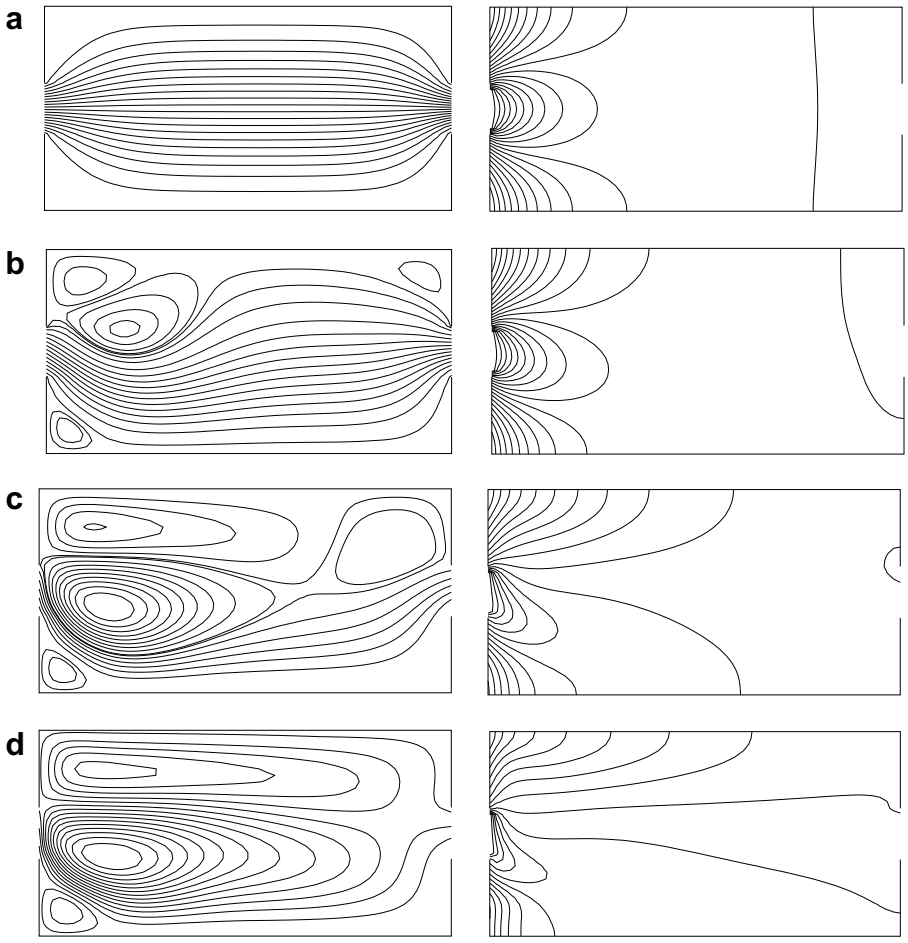

Fig. 3. Streamlines and isotherms obtained for $Re = 10$ and different values of Ra: (a) $Ra = 0$, (b) $Ra = 10^4$, (c) $Ra = 10^5$ and (d) $Ra = 5 \times 10^5$.

The basic forced convection flow, presented in Fig. 3a for $Ra = 0$, is characterized by a perfect symmetry of the solution with respect to the horizontal axis corresponding to $y = 0.5$ (horizontal axis passing by the mediums of the two openings). By increasing Ra to 10^4, Fig. 3b shows a big change in the flow structure; the symmetry already observed is destroyed and a multicellular flow arises causing a big deformation of the open lines, just below the two cells generated by the upper heated wall. The importance of the forced flow is visibly affected in Fig. 3c, corresponding to $Ra = 10^5$. The increase of the natural convection importance has supported the fusion of the two cells located just above the open lines to the detriment of the latter (open lines) what maintains the lower cell in a secondary role. More increase of Ra leads to more important cells above the open lines causing a visible tightening of these lines and showing a net domination of the natural convection effect, rather due to the heating of the higher portion of the left wall. Moreover, this increase of Ra contributes to the homogenisation of the temperature within the cavity by reducing the dimension of the cold zone, as it is shown by the isotherms. These aspects correspond to Fig. 3d, plotted for $Ra = 5 \times 10^5$.

From a practical point of view, the evaluation of mean and maximum temperatures of the fluid inside the cavity is of importance. Being inversely proportional to the heat flux q′, it appears more convenient to use a modified mean ($\overline{T}^* = \overline{T} \times Ra$) and maximum ($T^*_{\max} = T_{\max} \times Ra$) temperatures for these parameters to have the same tendencies as the corresponding real temperatures. In fact, variations of $\overline{T}$ and $T_{\max}$ present situations where they decrease by increasing Ra, which do not correspond to the tendencies of the real temperatures. Such observation was also formulated by Papanicolaou and Jaluria (1994) and Hsu et al. (1997). Thus, the variations versus Re, of the modified mean and maximum temperatures are presented in Fig. 4a–b for different values of Ra. For all considered values of Ra, Fig. 4a shows that $\overline{T}^*$ decreases by increasing Re, indicating that the overheat phenomenon is reduced for higher values of Re. Variations of the modified maximum temperature inside the cavity are presented in Fig. 4b. It can be seen that $T^*_{\max}$ decreases also by increasing Re, monotonously for $Ra = 10^4$ and towards a minimum (hardly visible) for higher values of Ra, reached for a critical value of Re corresponding to a maximum competition between natural and forced convections. The minimum of $T^*_{\max}$ is moved towards higher Re by increasing Ra.

The variations, with Re, of the normalized average Nusselt number, evaluated on the heated vertical wall, is

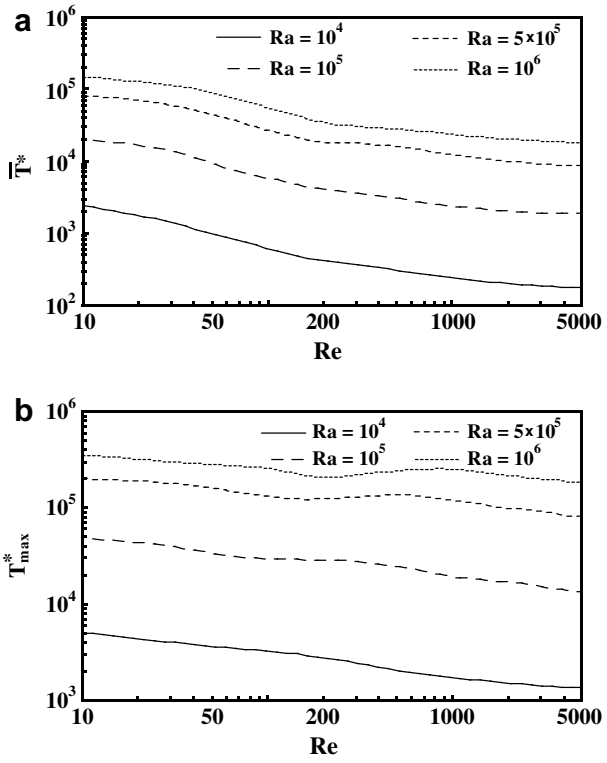

Fig. 4. Variations, with Re, of the modified mean, $\overline{T}^*$, and maximum, T^*_{max}, temperatures for different values of Ra.

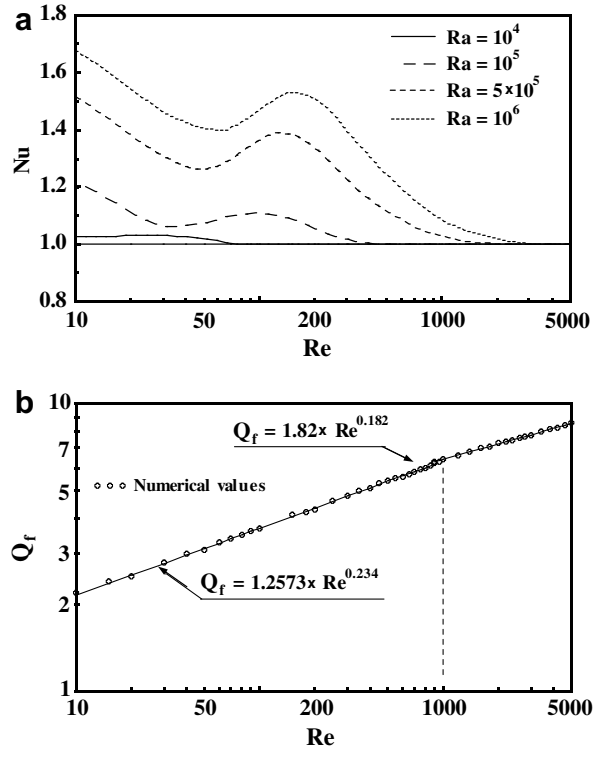

Fig. 5. Variations, with Re, of the normalized mean Nusselt number, Nu, and the quantity $Q(Ra = 0)$ for different values of Ra.

presented in Fig. 5a for various values of Ra. The normalization used for Nu (normalization with respect to conduction, $Ra = 0$, and forced convection, $Re \neq 0$) puts into evidence the contribution of natural convection compared to the basic flows obtained for $Ra = 0$. Generally, three tendencies, amplified by the increase of Ra, are observed. The increase of Re from its lower value leads first to a diminution of Nu towards a secondary minimum, followed by a change in the tendency (increase of Nu with Re towards a maximum) explained by a better interaction between forced and natural convection flows. Once the maximum is reached, a new change in the tendency, characterized by a continuous decrease of Nu towards unity (forced convection regime) is observed. The minimum and maximum values of Nu are reached for critical values of Re which depend on Ra. The values of $Q_f = Q$ $(Ra = 0)$, used in the normalization of Nu, are presented versus Re in Fig. 5b where a linear dependency can be observed. The numerical values of Q_f, used in the normalization of Nu, are correlated versus Re. The two correlations proposed, respectively, valid in the ranges $10 \leqslant Re \leqslant 1000$ and $1000 < Re \leqslant 5000$, agree with the numerical results with a maximum deviation of 1.5%.

The different flow regimes, identified in the present study, are delineated in the Ra–Re plane and presented in Fig. 6. The Reynolds number, Re_m, for which the competition between natural and forced convection generates maximum value of Nu, is seen to increase linearly with Ra in a logarithmic scale. The numerical values of Re_m are correlated as $Re_m = 3.7896 \times Ra^{0.2753}$. For a given value of Ra, the increase of Re above Re_m leads to a decrease of Nu towards unity; value reached for $Re = Re_f$. Further increase of Re from $Re_f = 0.0724 \times Ra^{0.7654}$, marks the total dominance of the forced convection. It is to note that the agreement between the numerical results (empty circles) and those corresponding to the correlations (solid lines) is seen to be excellent; the maximum deviation remains within 0.75%. The correlated critical values of Re allows simple and quick delimitations of the various flow regimes identified in the studied configuration. It is interesting to underline that for cavities subjected to the same thermal boundary conditions and provided with an inflow opening

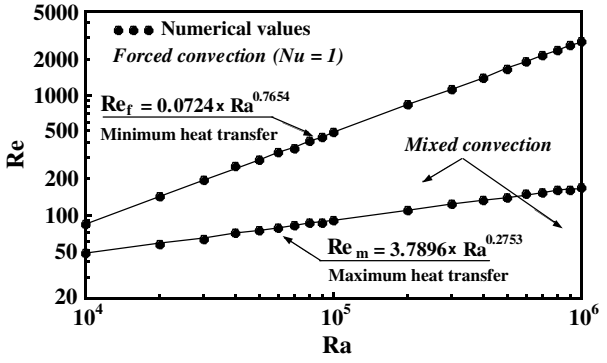

Fig. 6. Characterization of the existing flow regimes in the Ra–Re plane.

located at the lower part of the left vertical wall (Raji and Hasnaoui, 1998a) or at the level of its upper part (Raji and Hasnaoui, 1998b), the forced convection regime, corresponding to $Nu = 1$, could not be reached. Hence, in terms of cooling efficiency, the present configuration, compared to those described in Raji and Hasnaoui (1998a,b), allows most effective cooling conditions by maximizing the heat-removal rate and reducing the overall mean and maximum temperatures. In addition, a close comparison with results reported in these references shows that the maximum cooling effectiveness is achieved when the two openings are located at the middle of the vertical walls or when the inlet (outlet) is placed at the bottom (top) of the vertical heated (adiabatic) wall.

6. Conclusion

Mixed convection in a ventilated cavity, heated from its vertical left wall with a constant heat flux and thermally insulated from its remaining boundaries, was studied numerically using a finite difference method. The heat transfer generated by forced convection and used in the normalization of Nu was correlated as $Q\ (Ra = 0) = 1.2573 \times Re^{0.234}$ and $1.82 \times Re^{0.182}$ for $Re \leqslant 1000$ and $Re > 1000$, respectively. Results of the study show that the flow structure is considerably influenced by the interaction between natural convection (supported by the Rayleigh number) and forced convection (supported by the Reynolds number). The different flow regimes were identified and delineated in the Ra–Re plane. The couples (Ra, Re) leading to maximum Nu were identified and correlated as $Re_m = 3.7896 \times Ra^{0.2753}$. Above this limit of Re, the Nusselt number decreases monotonously towards $Nu = 1$; value marking the forced convection predominance. The values of Re from which $Nu = 1$, are also correlated as $Re_f = 0.0724 \times Ra^{0.7654}$.

References

Bhoite, M.T., Narasimham, G.S.V.L., Krishna Murthy, M.V., 2005. Mixed convection in a shallow enclosure with a series of heat generating components. Int. J. Therm. Sci. 44, 121–135.

De Vahl Davis, G., 1983. Natural convection of air in a square cavity: a benchmark numerical solution. Int. J. Numer. Meth. Fluids 3, 249–264.

Deng, Q.H., Zhou, J., Mei, C., Shen, Y.M., 2004. Fluid, heat and contaminant transport structures of laminar double-diffusive mixed convection in a two-dimensional ventilated enclosure. Int. J. Heat Mass Transfer 47, 5257–5269.

How, S.P., Hsu, T.H., 1998. Transient mixed convection in a partially divided enclosure. Comput. Math. Appl. 36, 95–115.

Hsu, T.H., Hsu, P.T., How, S.P., 1997. Mixed convection in a partially divided rectangular enclosure. Numer. Heat Transfer Part A 31, 655–683.

Hsu, T.H., Wang, S.G., 2000. Mixed convection in a rectangular enclosure with discrete heat sources. Numer. Heat Transfer Part A 38, 627–652.

Manca, O., Nardini, S., Khanafer, K., Vafai, K., 2003. Effect of heated wall position on mixed convection in a channel with an open cavity. Numer. Heat Transfer Part A 43, 259–282.

Oosthuizen, P.H., Paul, J.T., 1985. Mixed convective heat transfer in a cavity. ASME HTD 42, 159–169.

Papanicolaou, E., Jaluria, Y., 1990. Mixed convection from an isolated heat source in a rectangular enclosure. Numer. Heat Transfer Part A 18, 427–461.

Papanicolaou, E., Jaluria, Y., 1993. Mixed convection from a localized heat source in a cavity with conducting walls: a numerical study. Numer. Heat Transfer Part A 23, 463–484.

Papanicolaou, E., Jaluria, Y., 1994. Mixed convection from simulated electronic components at varying relative positions in a cavity. ASME J. Heat Transfer 116, 960–970.

Raji, A., Hasnaoui, M., 1998a. Mixed convection heat transfer in a rectangular cavity ventilated and heated from the side. Numer. Heat Transfer Part A 33, 533–548.

Raji, A., Hasnaoui, M., 1998b. Corrélations en convection mixte dans des cavités ventilées. Revue Générale de Thermique 37, 874–884.

Raji, A., Hasnaoui, M., 2000. Mixed convection heat transfer in ventilated cavities with opposing and assisting flows. Eng. Comput. Int. J. Comput.-Aided Eng. Softw. 17, 556–572.

Saha, S., Saha, G., Ali, M., Quamrul Islam, M., 2006. Combined free and forced convection inside a two-dimensional multiple ventilated rectangular enclosure. ARPN J. Eng. Appl. Sci. 1 (3), 23–35.

Singh, S., Sharif, M.A.R., 2003. Mixed convective cooling of a rectangular cavity with inlet and exit openings on differentially heated side walls. Numer. Heat Transfer Part A 44, 233–253.

Yücel, C., Hasnaoui, M., Robillard, L., Bilgen, E., 1993. Mixed convection heat transfer in open ended inclined channels with discrete isothermal heating. Numer. Heat Transfer 24, 109–126.